Virtual Screening and Prediction of Site of Metabolism for Cytochrome P450 1A2 Ligands

Poongavanam Vasanthanathan,[†,§] Jozef Hritz,[†] Olivier Taboureau,[¶] Lars Olsen,[§] Flemming Steen Jørgensen,[§] Nico P. E. Vermeulen,[†] and Chris Oostenbrink*[,†]

Leiden-Amsterdam Center for Drug Research, Section of Molecular Toxicology, Department of Chemistry and Pharmacochemistry, Vrije Universiteit, De Boelelaan 1083, 1081 HV, Amsterdam, The Netherlands, Biostructural Research, Department of Medicinal Chemistry, Faculty of Pharmaceutical Sciences, University of Copenhagen, Universitetsparken 2, DK-2100 Copenhagen, Denmark, and Chemoinformatics, BioCentrum-DTU, Technical University of Denmark, Building 208, DK-2800 Lyngby, Denmark

Received July 25, 2008

With the availability of an increasing number of high resolution 3D structures of human cytochrome P450 enzymes, structure-based modeling tools are more readily used. In this study we explore the possibilities of using docking and scoring experiments on cytochrome P450 1A2. Three different questions have been addressed: 1. Binding orientations and conformations were successfully predicted for various substrates. 2. A virtual screen was performed with satisfying enrichment rates. 3. A classification of individual compounds into active and inactive was performed. It was found that while docking can be used successfully to address the first two questions, it seems to be more difficult to perform the classification. Different scoring functions were included, and the well-characterized water molecule in the active site was included in various ways. Results are compared to experimental data and earlier classification data using machine learning methods. The possibilities and limitations of using structure-based drug design tools for cytochrome P450 1A2 come to light and are discussed.

INTRODUCTION

Cytochrome P450s (CYPs) form a superfamily of heme-thiolate containing proteins, which play a crucial role in the metabolism of endogenous and exogenous compounds. In total more than 250 different families of CYPs have been characterized; in mammals 18 families and 43 subfamilies have been reported.[1] In humans, CYPs contribute to 70−80% of the phase I metabolism of currently marketed drugs,[2,3] with the most important isoforms for metabolism being CYP1A2 (∼5% of current drugs), CYP2C9 and CYP2C19 (∼25%), CYP2D6 (∼15%), and CYP3A4 (∼50%).[3] Recent estimates suggest that the majority of drug candidate failures was due to poor pharmacokinetics and toxicity. Accordingly, the importance of early consideration of ADMET (absorption, distribution, metabolism, excretion, and toxicity) properties in the drug discovery process is currently strongly stressed.[4,5] CYPs play important roles both in the metabolism and the toxicity of drugs, drug candidates, or other xenobiotic chemicals, either through direct activation of reactive intermediates or through drug-drug interactions mediated by inhibition or induction of CYPs. As the importance of CYPs became clear, the interest in studying these protein systems both *in vitro* and *in silico* increased.[6−9]

Cytochrome P450 1A2 is responsible for the metabolism of many exogenous and endogenous compounds, such as caffeine, estradiol, naproxen, paracetamol, and theophylline. CYP1A2 enzyme is inducible by some polycyclic aromatic hydrocarbons (PAH) and heterocyclic amines, some of which are found in cigarette smoke and charred food. It can activate procarcinogens to carcinogens, and an overexpression of CYP1A2 has been linked to a high risk of colon cancer.[10]

The active site of CYP1A2 has been well characterized[11−14] as being narrow and lined by residues on helix F and helix I. Figure 1 shows 2D and 3D representations of the narrow, flat active site, which is formed mainly by the backbone of residues Gly316, Ala317, and Asp320. At the top of the site, there is an aromatic cluster formed by Phe226, Phe256, and Phe260. Aromatic substrates are believed to be sandwiched between the planar bottom and the aromatic top. Thr118, Ser122, and Thr124 are the main candidates to form polar contacts between the protein and the ligands. Residue Thr223 from helix H is involved in a strong hydrogen bond with Asp320 of helix I, and both residues are involved in an extensive network of hydrogen-bonded water molecules and side chains, including Tyr189, Val220, Thr498, and Lys500.

The X-ray structure with α-naphthoflavone (αNF) additionally shows a hydrogen bond between the inhibitor and one of these water molecules.[14] Substrates are characterized as neutral or basic, lipophilic, planar molecules with at least one putative hydrogen bond donating group.[13]

Experiments involving the binding of small compounds to the CYP1A2 enzyme can be rationalized or predicted by *in silico* tools at different levels of molecular description.[8] Previously we have successfully applied various machine learning techniques to discriminate CYP1A2 ligands from nonligands, and we have developed a simple Lipinski-based decision tree model, based on a library of 7469 compounds.[15]

* Corresponding author phone: +31205987606; fax: +31205987610; e-mail: c.oostenbrink@few.vu.nl.
[†] Vrije Universiteit.
[§] University of Copenhagen.
[¶] Technical University of Denmark.

10.1021/ci800371f CCC: $40.75
Published on Web 12/19/2008

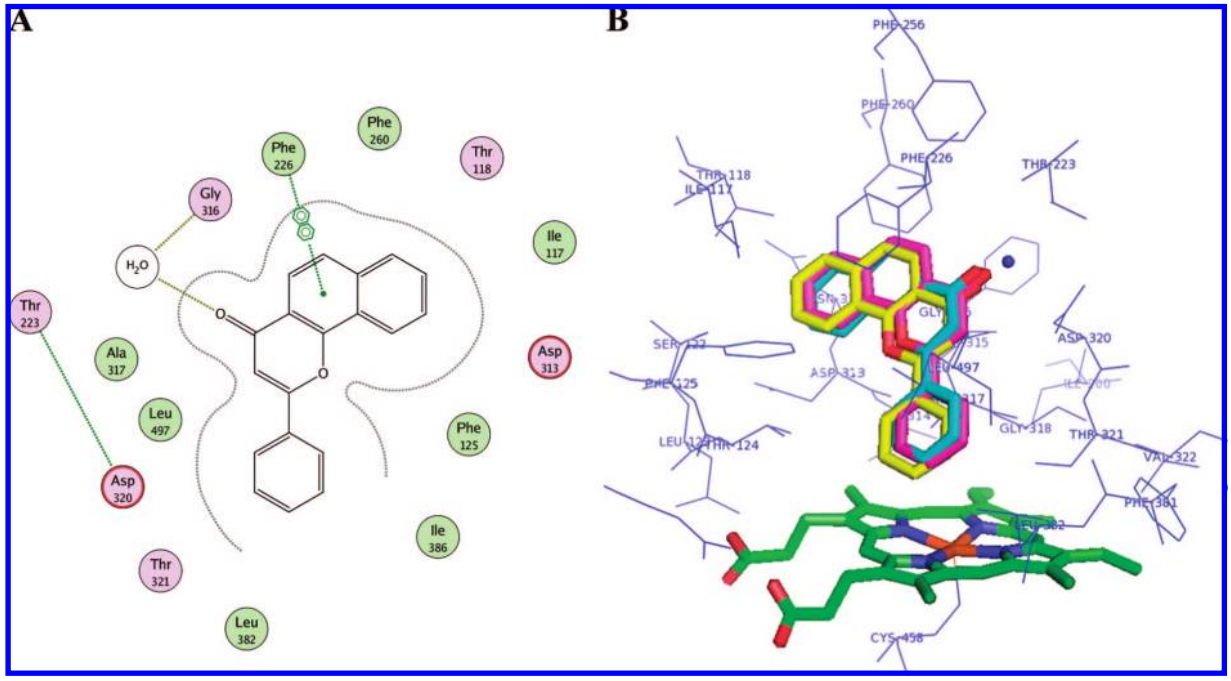

Figure 1. CYP1A2 active site with the inhibitor α-naphthoflavone (αNF) bound. A) Schematic representation of active site residues and αNF-protein interactions. B) 3D representation including the heme group (green), the active site water molecule (blue sphere), and αNF according to the X-ray structure (cyan); from docking without the active site water (scenario I; pink) and from docking in the presence of the active site water (scenario II; yellow).

These models are extremely fast and easy to use but lack molecular detail to describe the protein−ligand interactions. Structure-based drug design (SBDD) approaches are more suitable to offer such details. Previously, such techniques have been described for various studies on CYPs, such as site of metabolism prediction and virtual screens.[16−19] Here, we describe automated docking experiments on CYP1A2, using the same library of compounds as described before. In general, we distinguish between three kinds of questions that docking may address.

1. Prediction of the binding pose of a substrate or inhibitor. This provides detailed atomistic information about protein−ligand interactions and in the case of substrates may give insights into the possible site of metabolism (SOM).

2. Virtual screening to identify novel inhibitors or substrates from a large library of compounds. This is a typical application of docking in the drug discovery and design process and may help to find new inhibitors. As CYPs are more often considered to be an antitarget rather than a target, the practical applications of virtually screening large databases are limited.

3. Predicting binding affinities for individual compounds and accurately ranking several compounds with respect to each other. This may seem very similar to the second question but is different in a subtle way. In CYP research, one would not only like to find just any active compound from a library of compounds but one would also like to predict if any given compound is likely to be an inhibitor or not.

In the present study, we address the three questions outlined above using automated docking and structure-based virtual screening on 7469 compounds from the Pubchem bioassay database (AID: 410). These compounds are experimentally classified as inhibitors (4138 compounds) or noninhibitors (3331 compounds).[20] First, the docking strategies are validated to reproduce the X-ray complex, and binding poses are predicted for 20 substrates (Figure 2) and compared with the experimentally determined site of metabolism (SOM). Subsequently, virtual screening was performed by screening for 20 randomly selected active compounds and for the 20 substrates in Figure 2, which have been added to the set of 3331 inactive compounds. Finally, we determine if the scoring functions are able to distinguish the 4138 actives from the 3331 inactives and if the model is able to predict the activity for any given compound. Different scenarios involving the choice of scoring functions, consideration of different tautomers, and active site water molecules are investigated.

COMPUTATIONAL METHODS

Preparation of Protein and Ligands. The atomic coordinates of the human cytochrome P450 1A2 in complex with α-naphthoflavone (αNF) as obtained by X-ray crystallography[14] (1.95 Å resolution) were obtained from the Protein Data Bank (PDB ID 2H14). Hydrogen atoms were added using the MOE software (version 2007.09).[21]

A set of 7469 compounds, classified as active or inactive as inhibitor for CYP1A2, was collected from the Pubchem bioassay database.[20] 3D structures were generated using the Concord software[22] and imported into MOE to remove all counterions, solvent molecules, and salts in the structures. Protonation states according to a pH of 7 were assigned using the "Protonate 3D" option in MOE. Stereochemistry of the molecules was included in the SMILES notation of the Pubchem database. All molecules were energy minimized using the MMFF94 force field and subsequently exported into individual mol2 files using the *mdb2file*-script, kindly provided to us by the Chemical Computing Group. The 20 substrates shown in Figure 2 were first built in MOE, after which the same procedure was followed.

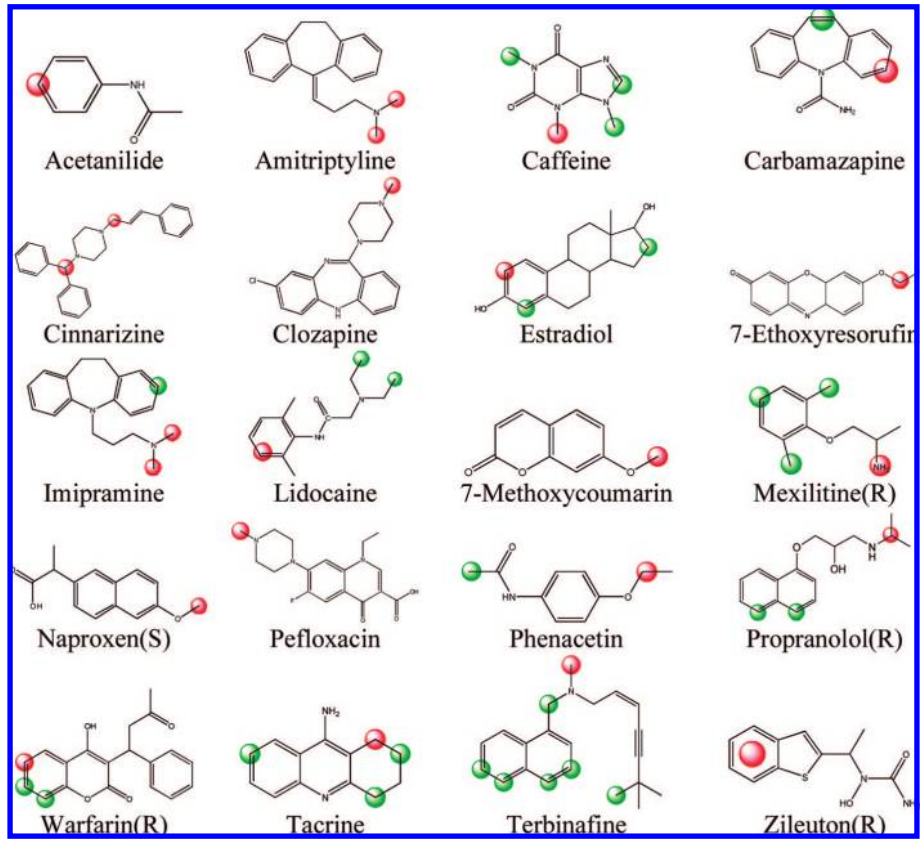

Figure 2. List of CYP1A2 substrates used for model validation. Red spheres indicate the most important experimentally measured site of metabolism; green spheres indicate minor metabolic sites. For references, see Table 2.

Table 1. Different Docking Scenarios Used in This Study

scenarios	scoring function	water[a]
I	Chemscore	off
II	Chemscore	on (spin)
III	Chemscore	toggle
IV	Goldscore	off
V	Goldscore	on (spin)
VI	Goldscore	toggle

[a] Refers to the crystallographic water molecule that mediates a hydrogen bond between the inhibitors and the protein.

Automated Docking Methodology. Gold version 3.2 (Genetic Optimization for Ligand Docking)[23] is a genetic algorithm for docking flexible ligands into protein binding sites. The program has the option to ignore or include specific water molecules during the docking procedure. Alternatively, Gold can automatically determine whether a specific water should be bound or displaced by turning its interactions on or off during the docking run (toggle). The orientation of the water hydrogen atoms can also be optimized by Gold by allowing the water molecule to spin.[24] In Gold, the docking may be guided by either the Goldscore or the Chemscore scoring functions. No additionally optimized parameter sets[25] for heme-containing proteins were used here, because we have successfully used the Gold- and Chemscore scoring functions for CYPs previously.[17] Table 1 shows the different docking scenarios that were considered in this study. Only the active site water molecule indicated in Figure 1 was turned off, spinned, or toggled. The radius for docking was set to 20 Å around a point in the center of the active site. Five docking runs and maximally 1000 operations were performed using a population of 100 genes. The genetic algorithm terminates on a given ligand if the top three solutions were obtained within 1.5 Å root-mean-square-deviation (rmsd).

Gold also offers the possibility to perform constrained docking, which was used for some of the substrates (see below). The distance between the heme iron and the experimentally observed site of metabolism (heavy atom) was restrained to be between 5 Å and 6 Å, using a force constant of 50 kJ/Å^2.

Analysis. Docking poses are evaluated in terms of their atom-positional root-mean-square-deviation (rmsd) with respect to a given reference or by calculating the proximity of experimentally observed sites of metabolism of substrates to the heme iron. As a rule of thumb, the pose of a substrate is considered to represent a catalytically active conformation if the site of metabolism is within 6 Å of the heme iron.[17] Virtual screening effectiveness is evaluated in terms of the enrichment factor (EF) as a function of the percentage x that is covered of the complete ranked database

$$EF(x) = f_{active}(x)/x \quad (1)$$

where f_{active} is the percentage of the actives found after assessing x% of the ranked database. The protein−ligand interactions of all compounds were analyzed using the Protein−Ligand Interaction Fingerprint (PLIF) module in MOE.[21] PLIF is a new tool included in MOE, using a fingerprint scheme consisting of 6 types of interactions. Hydrogen bonds, ionic interactions, and surface contacts are considered according to the residue of origin (backbone and side chain are distinguished separately). It is an effective way of dealing with large data sets. In our work, the first ranked docking poses were considered and analyzed using

Table 2. Metabolic Site Prediction for 6 Different Scenarios

				distance first ranked pose (Å)[a]						first rank within 6 Å[b]					
no.	compound	SOM (experiment)	ref	I	II	III	IV	V	VI	I	II	III	IV	V	VI
1	acetanilide	C-4 hydroxylation	44	4.7	4.4	4.6	10.8	8.6	8.5	1	1	1	-	-	-
2	amitriptyllin	N-demethylation	28, 45	4.6	11.1	11.8	4.6	5.2	5.2	1	2	3	1	1	1
3	caffeine	N3-demethylation	28	5.8	5.3	5.5	8.4	8.2	8.9	1	1	1	-	-	3
4	carbamazepine	hydroxylation at phenyl ring	46	7.5	8.0	7.9	8.1	7.1	6.8	-	2	3	-	-	-
5	cinnarizine	N-dealkylation	47	6.7	5.9	9.9	10.9	10.2	10.6	-	1	-	-	3	-
6	clozapine	N-dealkylation	48	7.6	7.7	8.6	7.7	8.4	9.1	-	-	-	-	-	-
7	estradiol	C-2 hydroxylation	49	4.7	4.4	11.1	4.8	4.2	4.2	1	1	2	1	1	1
8	7-ethoxyresorufin	O-deethylation	50	12.3	14.0	3.4	4.6	2.9	4.4	2	2	1	1	1	1
9	imipramine	N-demethylation	33	5.4	11.7	10.8	12.6	4.6	11.4	1	-	3	4	1	2
		C-2 hydroxylation		-	4.2	-	-	-	-	-	1	-	-	-	-
10	lidocaine	hydroxylation at phenyl ring	51	4.1	4.5	3.5	4.6	3.8	4.1	1	1	1	1	1	1
11	7-methoxycoumarin	O-demethylation	31	11.4	3.6	11.0	10.2	12.3	10.8	4	1	-	-	4	-
12	mexiletine	N-OH, OH at phenyl ring	52	4.5	4.8	12.3	12.2	8.9	9.4	1	1	2	2	4	-
13	naproxen (R)	O-demethylation	53	12.3	11.6	12.3	12.0	11.7	11.5	2	2	2	-	-	-
14	pefloxacin	N-demethylation	54	3.9	4.9	5.7	13.6	10.7	12.6	1	1	1	-	2	-
15	phenacetin	O-deethylation	55	4.3	4.7	5.8	11.1	4.1	5.1	1	1	1	4	1	1
16	propranolol (R)	N-deisopropylation	56	11.2	4.4	5.1	11.1	4.6	5.0	2	1	1	2	1	1
17	warfarin (R)	C-6 hydroxylation	57	4.3	5.9	4.6	4.8	6.0	4.7	1	1	1	1	1	1
18	tacrine	C-1 hydroxylation	58	4.7	5.2	4.9	5.8	6.1	5.7	1	1	1	1	3	1
19	terbinafine	N-demethylation	59	10.9	10.3	11.8	11.4	11.0	10.5	-	-	-	-	-	-
20	zileuton (R)	hydroxylation at phenyl ring	60	4.2	4.7	5.0	10.5	10.1	6.4	1	1	1	3	-	-

[a] Distances between the known site of metabolism indicated in Figure 2 and the heme iron. [b] First occurrence of a pose for which the distance between the site of metabolism and the heme iron is within 6 Å.

the PLIF module. We notice that π-π interactions are not integrated in the PLIF tool. As these interactions play an important role for CYP1A2, we estimated the relevance of the aromatic interactions by counting the number of compounds for which the first ranked pose displays an aromatic group within 3.5 Å of the midpoint between Phe226 and Phe260.

RESULTS AND DISCUSSION

As mentioned in the Introduction, docking experiments can be used to answer three questions. First, one may be interested in the position and orientation an inhibitor or substrate adopts. Second, one may attempt to identify compounds that have affinity for the protein from a large database of compounds. Third, one may want to predict for any given molecule whether or not it has affinity for the protein. Below, we will present and discuss our docking experiments to address these three issues for the CYP1A2 enzyme.

Validation of Ligand Binding Modes. An initial validation of the docking protocol is performed by comparing the conformation, position, and orientation (the *pose*) of the ligand α-naphthoflavone (αNF) as obtained from docking with the one determined experimentally with X-ray crystallography. Correctly redocking the crystallographically observed inhibitor is a minimum requirement to determine whether the program is applicable to this system or not. αNF was docked to the enzyme according to the 6 scenarios in Table 1. The root-mean-square-deviation (rmsd) was calculated between the X-ray cocrystallized conformation of αNF and the docking solutions. All six scenarios were able to produce docking poses with rmsd <1 Å from the X-ray structure within the top 5 ranked poses. For scenarios I, II, V, and VI the first ranked pose had a rmsd <1 Å. The scenarios involving the Chemscore scoring function generally performed slightly better, with several docking poses below 0.5 Å rmsd. The best docking pose, however, was obtained using scenario V, where the second ranked pose showed an rmsd of 0.34 Å. Interestingly, the only docking poses with rmsd <1 Å for scenarios III and VI did include the active site water molecule, even though good poses were also observed for scenarios I and IV in which the water was turned off (0.37 Å and 0.53 Å, respectively). Figure 1B shows the best docking poses using scenarios I and II compared to the X-ray structure.

Site of Metabolism Prediction (SOM). As a next step, we investigated the prediction of docking poses for a set of 20 known CYP 1A2 substrates selected from the literature (Figure 2). These substrates were randomly selected, where structurally very similar compounds were excluded, and the primary literature was traced to be sure of CYP1A2 metabolism. A docking pose was considered to be successful if the site of metabolism as indicated in Figure 2 is within 6 Å of the heme iron atom. Red and green spheres indicate major and minor metabolic sites, respectively. Some of these substrates are also substrates for other CYP isoforms. R-warfarin, for instance, is metabolized by CYP2C9,[26,27] while cinnarizine, clozapine, imipramine, and mexiletine are also metabolized by CYP2D6[28,29] and R-warfarin and zileuton are metabolized by CYP3A4 as well. In most cases, however, the site of metabolism and formation of metabolite is different between the different isoforms. For example, R-warfarin is hydroxylated at the 6 position by CYP1A2, while CYP3A4 hydroxylates R-warfarin at the 10 position and CYP2C9 at the 4′ position.[27,30] This regioselectivity implies that purely reactivity based methods, which use e.g. quantum mechanical calculations on the ligands to predict the most likely SOM, cannot be expected to work for all substrates. On the other hand, note that the docking pose alone can also not account completely for experimentally observed sites of metabolism, as the intrinsic reactivity of the various sites in the substrate will play an important role

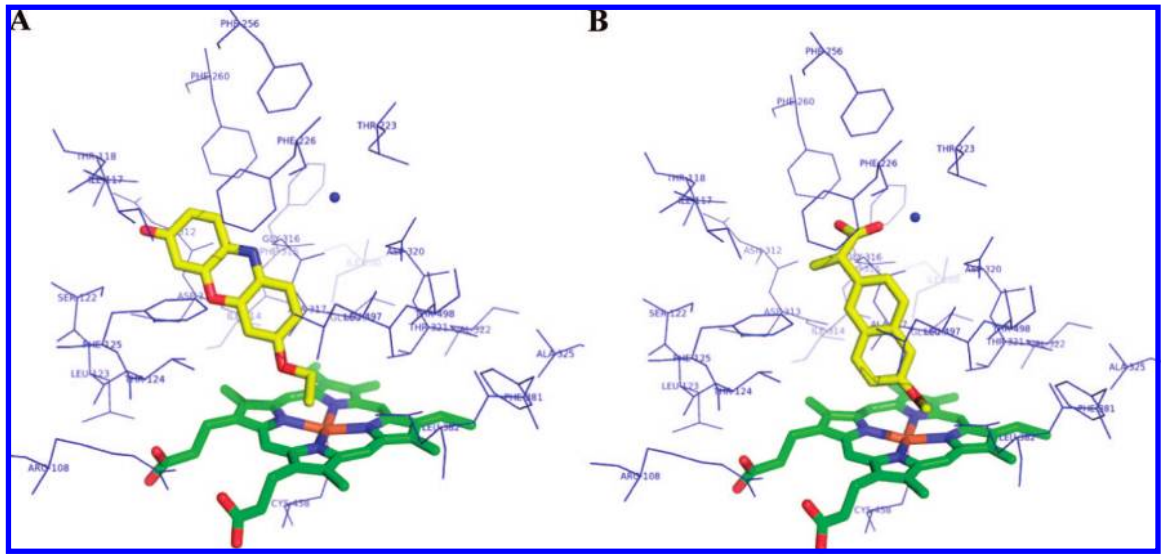

Figure 3. 7-Ethoxyresorufin (A) and naproxen (B) docked into the binding cavity of CYP1A2 by GOLD using scenario II. Important amino acid residues are highlighted in blue, water is depicted as a blue sphere, and the heme group is shown in green.

too.[16,31,32] However, as CYP1A2 displays one of the most restrictive CYP active sites, it is likely that the orientation induces a necessary requirement on observing a certain metabolite. The reactive pose still does not necessarily have to be the most prominent pose. For this reason we considered five different poses in this study. This is still a small enough number to allow for visual inspection.

The docking result for these substrates is summarized in Table 2 for all scenarios. In this table, the distance from the heme iron to the major site of metabolism of the substrates for the first ranked pose is given as well as the rank number for the first pose in which this value is below 6 Å. A dash (-) indicates that no such pose was found among the first 5 ranked poses. Note that for imipramine, a row was included in Table 2 for the minor metabolite as well, as will be discussed below.

The Chemscore scenarios I, II, and III were unsuccessful for 4, 3, and 4 compounds, respectively, and showed a successful first-ranked pose for 12, 13, and 10 compounds, respectively. The Goldscore scenarios IV, V, and VI were unsuccessful for 9, 7, and 9 compounds and showed a significantly lower number of successful first-ranked poses, being 6, 8, and 8, respectively. Possibly, the lack of explicit hydrophobic terms in Goldscore offers an explanation for this observation, as hydrophobic interactions are known to play a significant role for CYPs. Inclusion of the water molecules (scenarios II and V) improves the results slightly. With both scoring functions, two more compounds could be docked correctly, and the number of successful first-ranked poses increased slightly when compared to having the water turned off (scenarios I and IV). Giving the program the freedom to decide on the presence or absence of the water molecule (toggle; scenarios III and VI) would in theory improve the docking poses further, but this was not observed. For Chemscore (scenario III) the number of successful first-ranked poses decreased, while for Goldscore (scenario VI) the number of failed compounds even increased to 9 again. Figure 3 shows the successful docking poses for the CYP1A2 model substrate 7-ethoxyresorufin and for naproxen using docking scenario II. The poses are in accordance with the experimentally observed O-deethylation and O-demethylation of these compounds. The carbonyl oxygen of naproxen is involved in hydrogen bonding with the active site water molecule. Like in the X-ray structure with αNF, the water molecule can mediate the interactions between the substrate and the protein and thus stabilize the protein−ligand complex. However, the influence of the water molecule in the substrate binding of CYP1A2 is not so straightforward, as becomes clear from Figure 4. Imipramine is a tricyclic antidepressant drug primarily N-dealkylated by CYP1A2 but aromatically hydroxylated at C2 as well.[33] Figure 4 shows the first ranked poses according to the docking scenarios I, II, and III. Without the active site water molecule the major metabolite is correctly predicted. This pose was never observed when the water molecule was switched on (scenario II, Figure 4B), but rather poses corresponding to the minor metabolite were observed. Using the toggle option on the water molecule gives both docking poses; the first two ranked docking poses are similar to Figure 4C, while the third, fourth, and fifth docking poses again correspond to major metabolite formation (Figure 4A). Interestingly, Gold predicts the water molecule to be absent in all five poses. Possibly the maximum number of operations (1000) should be increased when the spin or toggle option for water is used, as this introduces additional degrees of freedom that need to be sampled by the genetic algorithm. On the other hand, for high-throughput virtual screening purposes, the docking efficiency (which increases with the number of operations) is crucial.

In the case of carbamazapine, cinnarizine, and terbinafine, the site of metabolism is correctly oriented toward the heme, but these molecules are often far away from the heme iron atom. A constrained docking run in which the site of metabolism was constrained to be within 6 Å of the heme iron showed for all four compounds that the active site does offer enough space for correct poses, but these were only seldomly observed in free docking runs.

Most of the 20 substrates were positioned on the flat surface of Gly316 and Ala317 and were involved in π-π interactions being placed between three phenylalanine rings (226, 256, and 260) as observed experimentally for αNF.[14]

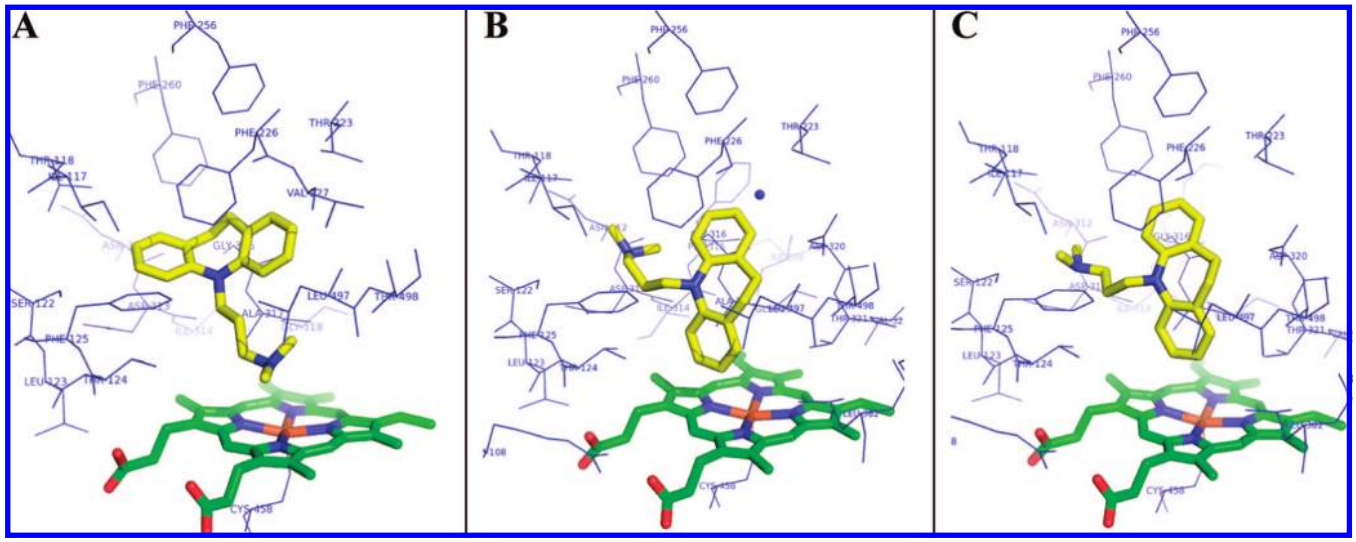

Figure 4. Comparison of imipramine metabolism prediction of docking without (A), with water (B), and toggle (C) of first ranked pose. Color representation of molecules is as follows: water-blue sphere, imipramine yellow stick model, heme green stick model, and important residues are depicted in blue lines.

Virtual Screening. The second question addresses virtual screening for novel inhibitors or substrates from a large compound library. This will help in the early drug discovery process to identify new or previously unknown inhibitors or substrates for specific isoforms. In this context, a small number of known ligands are added to a library of inactive compounds, and all are docked into the active site and scored. After sorting the compounds based on their scores, an enrichment analysis can be performed using eq 1. We determined the number of known actives screened from inactive compounds at different percentages of database coverage for various docking scenarios. From the enrichment analysis, one may determine the percentage at which a considerable number of actives can be expected to be identified. Here, 20 substrates (Figure 2) and 20 randomly selected inhibitors from the Pubchem database were used together with 3331 compounds listed as inactive. The effect of the active site water molecule seemed limited, so for clarity we restrict ourselves to scenarios I and IV. Figure 5 and Table 3 show the enrichment for both scenarios and both classes of compounds. Enrichment factors of 3−8 at 5% database coverage are on the low side but commonly reported.[17,34,35] The performance of Chemscore is better than Goldscore for both the substrates and the inhibitors. Especially for the substrates at 5 and 10% database coverage, Chemscore performs best for the substrates, with enrichment factors of 8.

As was mentioned in the Introduction, CYPs are often considered to be antitargets, rather than virtual screening targets, making it of less importance to search for novel inhibitors for these enzymes. Examples of coadministration of CYP inhibitors to prevent the formation of e.g. carcinogenic metabolites from other drugs are known,[36] but the field is highly regulated, and it is unlikely that one would screen for novel compounds as inhibitors for this purpose.

Activity Prediction. The third kind of question is of more interest for CYP research. It involves the prediction of binding affinities for individual compounds and the accurate ranking of several compounds with respect to each other. Determining if a compound is active or inactive is more difficult than screening for some (any) actives in a set of inactives. The prediction of binding affinity is still a major challenge in drug research. Here, we tried to classify active and inactive compounds based on their docking scores, using the different scenarios mentioned in Table 1. For clarity we present only scenarios I−IV. Figure 6 (Table 4) shows the comparison of the Chemscore/Goldscore for actives and inactives with and without water molecule. The values of the specificity and sensitivity in Table 4 represent the

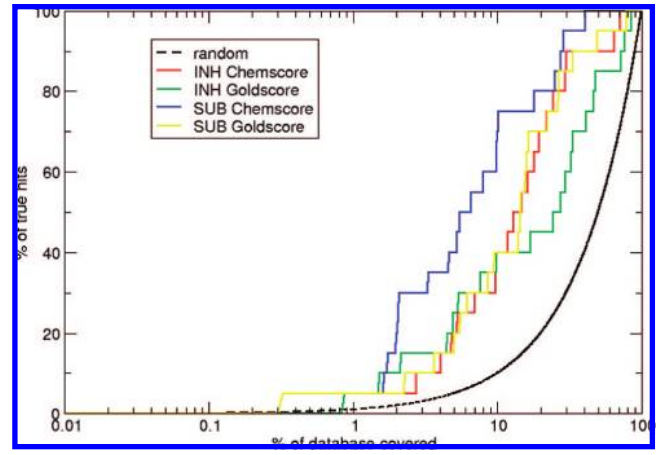

Figure 5. Enrichment plot of screening for the 20 substrates (Figure 2) and 20 randomly selected active compounds from the Pubchem database in a pool of 3331 inactive compounds from the Pubchem database. Red curve: screen for inhibitors using Chemscore; green curve: screen for inhibitors using Goldscore; dark blue curve: screen for substrates using Chemscore; cyan curve: screen for substrates using Goldscore; black curve: random picking.

Table 3. Number of Validation Compounds Found in Virtual Screening When Considering Different Percentages of the Total Database of 3351 Compounds[a]

		recall					
data set	scenarios	1%	5%	10%	25%	50%	100%
20 substrates	scenario I	1(5)	8(8)	14(8)	16(3)	20(2)	20(1)
20 substrates	scenario IV	1(5)	3(3)	9(5)	15(3)	19(2)	20(1)
20 inhibitors	scenario I	1(5)	4(4)	8(4)	16(3)	18(2)	20(1)
20 inhibitors	scenario IV	1(5)	5(5)	8(4)	10(2)	17(2)	20(1)

[a] In brackets, the enrichment factors according to eq 1 are given.

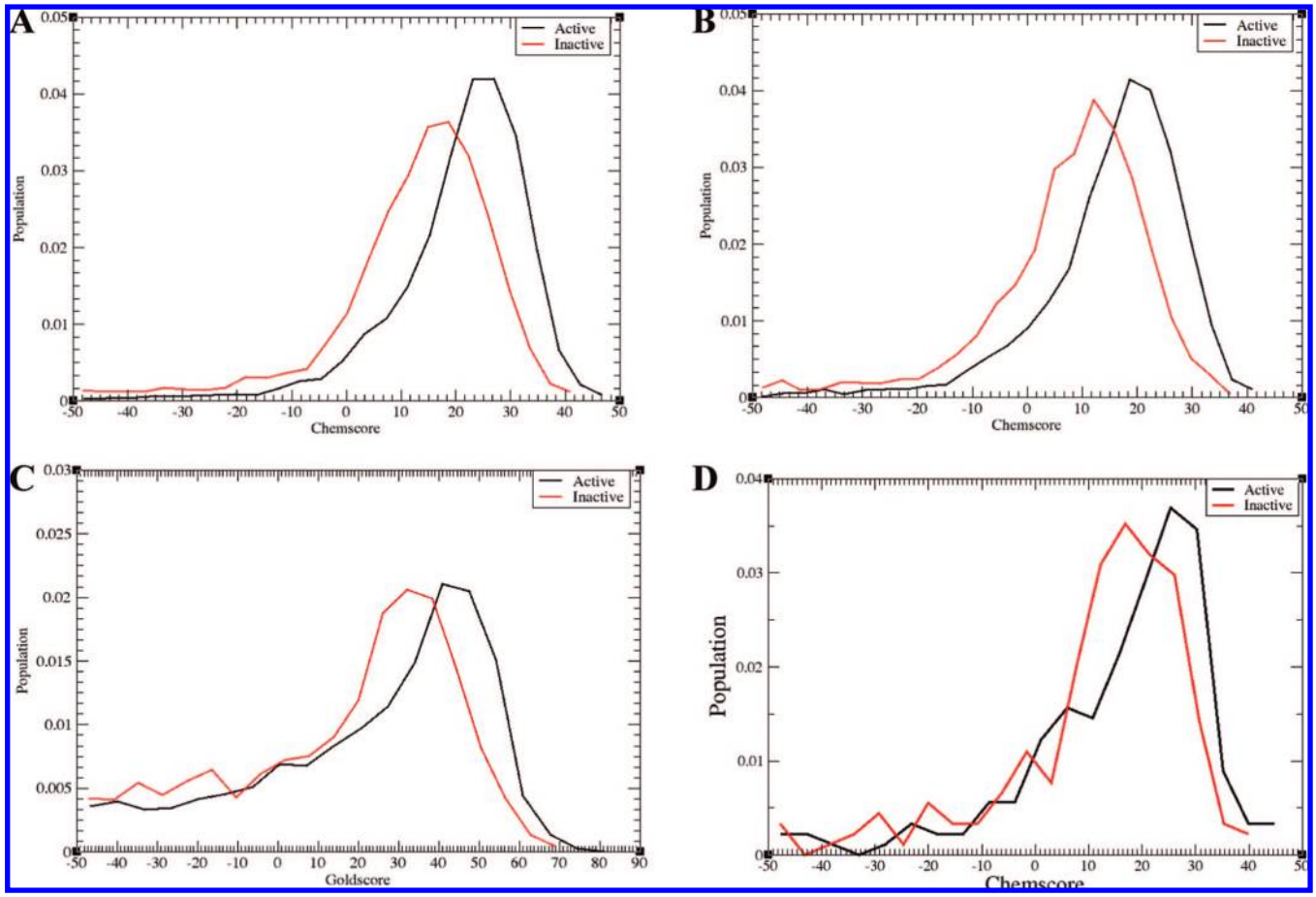

Figure 6. Distribution of active and inactive compounds by various docking scenarios: A) scenario I; B) scenario II; C) scenario IV; and D) training set of 411 compounds, scenario I.

Table 4. Summary of Classification of the Pubchem Database into Active and Inactive Compounds

	prediction[a]				
methods	TP	FN	FP	TN	κ index
scenario I	2524 (61)	1614	1066	2265 (68)	0.286
scenario II	2400 (58)	1738	966	2365 (71)	0.284
scenario III	2565 (62)	1573	1033	2298 (69)	0.305
scenario IV	1655 (40)	2483	833	2498 (75)	0.143
machine learning: Random forest[b]	3112 (78)	1026	685	2646 (76)	0.541

[a] TP: True positive; TN: True negative; FN: False negative; FP: False positive. Sensitivity = TP/(TP+FN)*100%; specificity = TN/(TN+FP)*100%; these values are given in brackets in the columns for TP and TN. [b] Data taken from ref 15.

percentage of inactive compounds with scores less than the intersection point of the two curves and the percentage of active compounds with scores larger than the intersection point. Those numbers may be interpreted as the successful classifications using the given cutoff score. Following the work of Chohan et al., we have also calculated the κ-index as a measure for the overall agreement for the classification. Following their interpretation, the values in Table 4 indicate a poor to fair agreement.[37] In Figure 6A,B a clear separation between active and inactive compounds can be seen for scenarios I and II, respectively. The ranges of inactive scores in both scenarios are similar, but the range for active scores varies. This leads to a slightly worse prediction of active compounds from 61% to 58%. When considering the water molecule using the toggle option in scenario III this prediction improves to 62% again. Docking without the active site water molecule using Goldscore (scenario IV; Figure 6C) shows that many compounds fail to dock with reasonable scores altogether leading to a very low prediction of actives (40%). In an additional experiment, all possible tautomers of the compounds in the library were generated using the program Agent3.2,[38] and the best ranked tautomer per compound was used to make the distributions of the scoring functions. No significant differences with the data in Figure 6 and Table 4 could be observed (data not shown).

In the Methods section, we have mentioned that the Pubchem data were already used for ligand-based classification by separating the whole data (7469 compounds) into training (411 compounds) and test set (7058) by a D-optimal onion design (DOOD). From the training set, machine learning methods could be obtained that were predictive for ~75% on the test set.[15] In order for the current structure-based approach to be applicable, one would need to determine a suitable score-cutoff to classify compounds as active or inactive from a similar training set. Using the same 411 compounds as before, the separation in Figure 6D was obtained for scenario I, with a prediction of actives of 45% and of inactives of 72%. This is clearly not good enough for a correct classification. Applying the cutoff of 22.2 from the training set to the complete data set leads to a correct prediction of only 55% of actives and 75% of the inactives, which clearly indicates that too many compounds are

considered to be inactive. To be predictive a more balanced number of true positives and true negatives should be obtained.

The separation between actives and inactives seen for scenarios I, II, and III only becomes apparent for large numbers of compounds and not for the training set of only 411 molecules with 192 active and 219 inactive compounds (Figure 6D). In general, the overall classifications based on the docking results are not as good as previously reported ligand-based models. Possible reasons for the failure of docking methods may be the fact that the protein conformation is considered to be rigid in the docking experiments. If inhibitors bind to different conformations of the protein, these may not be recognized as active compounds here. The lack of protein flexibility in docking experiments is a well-known challenge for structure-based drug design, which may be even more pronounced for CYPs, which are known to show a high level of plasticity allowing them to accommodate a large variety of substrates.[39] Another possible molecular explanation may be that the structure-based models assume that all inhibitors bind to the same active site, while machine learning methods may also be able to describe noncompetitive, allosteric inhibitors.

On the other hand, it has been observed previously that scoring functions do not correlate well with individual binding affinities of the compounds.[40−42] This, again, may also be attributed to the lack of protein flexibility and thus of an inaccurate description of the entropic contributions to the binding free energy. Moreover, affinities for CYPs are generally lower than for regular target proteins. It is well possible that it is more difficult to predict low affinity binding than high affinity binding.

Structural Information. Structure-based drug design approaches, such as automated docking, take the protein−ligand interactions explicitly into account. Ligand-based methods, like 2D/3D-QSAR, quantum mechanics-based calculations, pharmacophore modeling, and nonlinear machine learning methods do not have access to this information. The docking procedure proposes energetically favorable conformations and orientations of ligands in the binding pocket of a protein and predicts key interactions. In the present study, we have shown that docking may be used to give information about the bioactive conformation and may help to predict the metabolism of given substrates. From the docking study one may predict which positions in the substrate may be accessible for metabolization (site of metabolism prediction). An additional analysis can be performed to define which residues and which types of interactions are involved in the binding of the ligands. To do so, we performed a PLIF (Protein−Ligand Interaction Fingerprint) analysis which is implemented in the MOE software, in order to characterize the active site and the relevant interactions. Only compounds with docking scores >0 in scenario II were taken into account (5951 compounds). PLIF was generated on the active set of (3643) compounds and on the inactive set of (2308) compounds in order to capture the major features to distinguish substrates or inhibitors from inactives. For the active compounds (Figure 7), polar interactions are in majority mediated by Thr124 (43%). This residue was previously reported to have a major role in the interaction of substrates.[43] Additional polar interactions with Asp313 (17%) and Thr118 (12%) are also

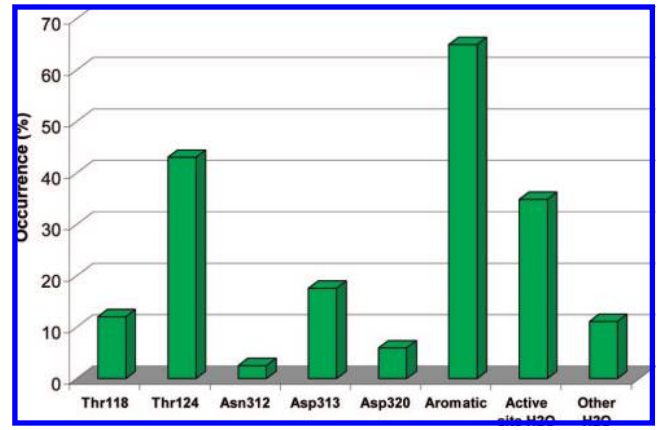

Figure 7. Occurrence of ligand-protein interactions with specific residues or groups in the CYP1A2 active site, for inactive compounds. Aromatic refers to interactions with the aromatic cluster made up of Phe226, Phe256, and Phe260. Other H2O refers to all water molecules other than the one indicated in Figure 1 (active site H2O).

significantly present with this set of ligands, which is in line with the description of the active site in the introduction and Figure 1A. Interestingly, 35% of the compounds show an interaction with the active site water molecule as indicated in Figure 1, while 11% have interactions with various other water molecules (none of which show interactions with >5% of the ligands). Aromatic interactions are mediated by Phe226, Phe256, and Phe260 for 65% of the ligands. When performing the same analysis for the 2308 inactive compounds, we note that the aromatic interaction is reduced to 44% of the compounds. Likewise, only 23% of the inactives show an interaction with the active site water molecule. Rather, the interactions with Asn312, Asp313, and Asp320 are increased, most notably for Asp313, to 28%. It seems that when inactive molecules are fitted into the active site of CYP1A2 anyway, they do not find the interactions important for actives but rather interact with these three residues in helix I that are to the left of the aromatic cluster in Figure 1B.

CONCLUSION

Various docking experiments have been performed for substrates and inhibitors of cytochrome P450 1A2 (CYP1A2). Various scenarios involving different scoring functions and the presence or absence of water molecules were included in the experiments. It turns out that this setup does allow for the identification of binding conformations and positions of various compounds and that also virtual screening experiments can be performed to identify active compounds from a database of mostly inactive ones. For a classification of individual compounds as actives or inactives, the scoring functions seem to perform less well than e.g. machine learning methods. A protein−ligand interaction fingerprint (PLIF) analysis performed on docking poses allows for an automatic and fast visualization of the occurrence of specific interactions. From this a molecular view on the most important interactions for CYP1A2 activity could be derived.

This work emphasized the possibilities and limitations of docking and scoring experiments in general and for CYP1A2 in particular. It is clear that for the accurate ranking of binding affinities, more elaborate methods will be required,

but the various docking scenarios performed well on the prediction of docking poses, which in turn leads to valuable insights concerning the molecular mechanism of this metabolic enzyme.

Abbreviations. ADMET, absorption, distribution, metabolism, excretion, and toxicity; αNF, α-naphthoflavone; CYP1A2, cytochrome P450 1A2 isoform; GA, genetic algorithm; Gold, genetic optimization for ligand docking; HTS, high throughput screening; MOE, molecular operating environment; PLIF, protein−ligand interaction fingerprint; QSAR, quantitative-structure activity relationship; rmsd, root mean square deviation; SBDD, structure-based drug design; SOM, site of metabolism; VS, virtual screening.

ACKNOWLEDGMENT

Authors P.V., L.O., and O.T. gratefully acknowledge the financial assistance provided by the *Drug Research Academy*, Faculty of Pharmaceutical Sciences, University of Copenhagen and the *Carlsberg Foundation*, and *NABIIT* (Nanoscience Biotechnology and IT) program, respectively. C.O. gratefully acknowledges the *Netherlands Organization for Scientific Research*, VENI Grant No. 700.55.401 for financial support.

REFERENCES AND NOTES

(1) Cytochrome P450 homepage. http://drnelson.utmem.edu/CytochromeP450.html (accessed July 2007).
(2) Bertz, R. J.; Granneman, G. R. Use of in vitro and in vivo data to estimate the likelihood of metabolic pharmacokinetic interactions. *Clin. Pharmacokinet.* **1997**, *3*, 210–258.
(3) Williams, J. A.; Hyland, R.; Jones, B. C.; Smith, D. A.; Hurst, S.; Goosen, T. C.; Peterkin, V.; Koup, J. R.; Ball, S. E. Drug-drug interactions for UDP-glucuronosyltransferase substrates: A pharmacokinetic explanation for typically observed low exposure (AUCi/AUC) ratios. *Drug Metab. Dispos.* **2004**, *32*, 1201–1208.
(4) DiMasi, J. A. New drug development in the United States from 1963 to 1999. *Clin. Pharmacol. Ther. (N. Y., NY, U. S.)* **2001**, 286–296.
(5) van de Waterbeemd, H.; Gifford, E. ADMET in silico modelling: towards prediction paradise. *Nat. Rev. Drug Discovery* **2003**, *2*, 192–204.
(6) de Graaf, C.; Vermeulen, N. P. E.; Feenstra, K. A. Cytochrome P450 in silico: an integrative modeling approach. *J. Med. Chem.* **2005**, *48*, 2725–2755.
(7) Baranczewski, P.; Stanczak, A.; Sundberg, K.; Svensson, R.; Wallin, A.; Jansson, J.; Garberg, P.; Postlind, H. Introduction to in vitro estimation of metabolic stability and drug interactions of new chemical entities in drug discovery and development. *Pharmacol. Rep.* **2006**, *58*, 453–472.
(8) Stjernschantz, E.; Vermeulen, N. P. E.; Oostenbrink, C. Computational prediction of drug binding and rationalisation of selectivity towards cytochromes P450. *Exp. Opin. Drug Metab. Tox.* **2008**, *4*, 513–527.
(9) Guengerich, F. P. Cytochrome P450 and chemical toxicology. *Chem. Res. Toxicol.* **2008**, *21*, 70–83.
(10) Kim, D.; Guengerich, F. P. Cytochrome P450 activation of arylamines and heterocyclic amines. *Annu. Rev. Pharmacol. Toxicol.* **2005**, *45*, 27–49.
(11) Smith, D. A.; Ackland, M. J.; Jones, B. C. Properties of cytochrome P450 isoenzymes and their substrates part 1: active site characteristics. *Drug Discovery Today* **1997**, *2*, 406–414.
(12) Smith, D. A.; Ackland, M. J.; Jones, B. C. Properties of cytochrome P450 isoenzymes and their substrates part 2: properties of cytochrome P450 substrates. *Drug Discovery Today* **1997**, *2*, 479–486.
(13) Ekins, S.; de Groot, M. J.; Jones, J. P. Pharmacophore and three-dimensional quantitative structure activity relationship methods for modeling cytochrome P450 active sites. *Drug Metab. Dispos.* **2001**, *29*, 936–944.
(14) Sansen, S.; Yano, J. K.; Reynald, R. L.; Schoch, G. A.; Griffin, K. J.; Stout, C. D.; Johnson, E. F. Adaptations for the oxidation of polycyclic aromatic hydrocarbons exhibited by the structure of human P450 1A2. *J. Biol. Chem.* **2007**, *282*, 14348–14355.
(15) Vasanthanathan, P.; Taboureau, O.; Oostenbrink, C.; Vermeulen, N. P. E.; Olsen, L.; Jørgensen, F. S. Classification of cytochrome P450 1A2 inhibitors and non-inhibitors by machine learning techniques. *Drug Metab. Dispos.* **2008**, DOI: 10.1124/dmd.108.023507.
(16) Afzelius, L.; Arnby, C. H.; Broo, A.; Carlsson, L.; Isaksson, C.; Jurva, U.; Kjellander, B.; Kolmodin, K.; Nilsson, K.; Raubacher, F.; Weidolf, L. State-of-the-art tools for computational site of metabolism predictions: comparative analysis, mechanistical insights, and future applications. *Drug Metab. Rev.* **2007**, *39*, 61–86.
(17) de Graaf, C.; Oostenbrink, C.; Keizers, P. H.; van der, W. T.; Jongejan, A.; Vermeulen, N. P. E. Catalytic site prediction and virtual screening of cytochrome P450 2D6 substrates by consideration of water and rescoring in automated docking. *J. Med. Chem.* **2006**, *49*, 2417–2430.
(18) De, R. F.; Fanelli, F.; Menziani, M. C.; De Benedetti, P. G. Theoretical investigation of substrate specificity for cytochromes P450 IA2, P450 IID6 and P450 IIIA4. *J. Comput.-Aided Mol. Des.* **2000**, *14*, 93–116.
(19) Locuson, C. W.; Gannett, P. M.; Ayscue, R.; Tracy, T. S. Use of simple docking methods to screen a virtual library for heteroactivators of cytochrome P450 2C9. *J. Med. Chem.* **2007**, *50*, 1158–1165.
(20) Pubchem bioassay Web site. http://pubchem.ncbi.nlm.nih.gov (accessed July 2007).
(21) *MOE (version 2007 09)*; Chemical Computing Group Inc.: 1010 Sherbrooke Street West, Suite 910, Montreal, Quebec, Canada H3A 2R7, 2007.
(22) *Concord (version 6.1.2)*; accessed via SYBYL (version 7.0) from Tripos Associates Inc.: St. Louis, U.S.A., 2007.
(23) Jones, G.; Willett, P.; Glen, R. C.; Leach, A. R.; Taylor, R. Development and validation of a genetic algorithm for flexible docking. *J. Mol. Biol.* **1997**, *267*, 727–748.
(24) Verdonk, M. L.; Chessari, G.; Cole, J. C.; Hartshorn, M. J.; Murray, C. W.; Nissink, J. W. M.; Taylor, R. D.; Taylor, R. Modeling water molecules in protein-ligand docking using GOLD. *J. Med. Chem.* **2005**, *48*, 6504–6515.
(25) Kirton, S. B.; Murray, C. W.; Verdonk, M. L.; Taylor, R. D. Prediction of binding modes for ligands in the cytochromes P450 and other heme-containing proteins. *Proteins* **2005**, *58*, 836–844.
(26) Mancy, A.; Antignac, M.; Minoletti, C.; Dijols, S.; Mouries, V.; Duong, N. T.; Battioni, P.; Dansette, P. M.; Mansuy, D. Diclofenac and its derivatives as tools for studying human cytochromes P450 active sites: particular efficiency and regioselectivity of P450 2Cs. *Biochemistry* **1999**, *38*, 14264–14270.
(27) Kaminsky, L. S.; Zhang, Z. Y. Human P450 Metabolism of warfarin. *Pharmacol. Ther.* **1997**, *73*, 7–74.
(28) Rendic, S. Summary of information on human CYP enzymes: human P450 metabolism data. *Drug Metab. Rev.* **2002**, *34*, 83–448.
(29) Nakajima, M.; Kobayashi, K.; Shimada, N.; Tokudome, S.; Yamamoto, T.; Kuroiwa, Y. Involvement of CYP1A2 in mexiletine metabolism. *Br. J. Clin. Pharmacol.* **1998**, *46*, 55–62.
(30) Rettie, A. E.; Korzekwa, K. R.; Kunze, K. L.; Lawrence, R. F.; Eddy, A. C.; Aoyama, T.; Gelboin, H. V.; Gonzalez, F. J.; Trager, W. F. Hydroxylation of warfarin by human cDNA-expressed cytochrome P-450: a role for P-4502C9 in the etiology of (S)-warfarin-drug interactions. *Chem. Res. Toxicol.* **1992**, *5*, 54–59.
(31) Jung, J.; Kim, N. D.; Kim, S. Y.; Choi, I.; Cho, K. H.; Oh, W. S.; Kim, D. N.; No, K. T. Regioselectivity prediction of CYP1A2-mediated phase I metabolism. *J. Chem. Inf. Model.* **2008**, *48*, 1074–1080.
(32) Feenstra, K. A.; Hofstetter, K.; Bosch, R.; Schmid, A.; Commandeur, J. N. M.; Vermeulen, N. P. E. Enantioselective substrate binding in a monooxygenase protein model by molecular dynamics and docking. *Biophys. J.* **2006**, *91*, 3206–3216.
(33) Koyama, E.; Chiba, K.; Tani, M.; Ishizaki, T. Reappraisal of human CYP isoforms involved in imipramine N-demethylation and 2-hydroxylation: A study using microsomes obtained from putative extensive and poor metabolizers of S-mephenytoin and eleven recombinant human CYPs. *J. Pharmacol. Exp. Ther.* **1997**, *281*, 1199–1210.
(34) Bender, A.; Glen, R. C. A discussion of measures of enrichment in virtual screening: comparing the information content of descriptors with increasing levels of sophistication. *J. Chem. Inf. Model.* **2005**, *45*, 1369–1375.
(35) Verdonk, M. L.; Berdini, V.; Hartshorn, M. J.; Mooij, W. T.; Murray, C. W.; Taylor, R. D.; Watson, P. Virtual screening using protein-ligand docking: avoiding artificial enrichment. *J. Chem. Inf. Comput. Sci.* **2004**, *44*, 793–806.
(36) Lamb, D. C.; Waterman, M. R.; Kelly, S. L.; Guengerich, F. P. Cytochromes P450 and drug discovery. *Curr. Opin. Biotechnol.* **2007**, *18*, 504–512.
(37) Chohan, K. K.; Paine, S. W.; Mistry, J.; Barton, P.; Davis, A. M. A rapid computational filter for cytochrome P450 1A2 inhibition potential of compound libraries. *J. Med. Chem.* **2005**, *48*, 5154–5161.

(38) Posposil, P.; Ballmer, P.; Scapozza, L.; Folkers, G. Tautomerism in computer-aided drug design. *J. Recept. Signal Transduction* **2003**, *23*, 361–371.

(39) Guengerich, F. P. A malleable catalyst dominates the metabolism of drugs. *Proc. Natl. Acad. Sci. U.S.A.* **2006**, *103*, 13565–13566.

(40) Ferrara, P.; Gohlke, H.; Price, D. J.; Klebe, G.; Brooks, C. L. III Assessing scoring functions for protein-ligand interactions. *J. Med. Chem.* **2004**, *47*, 3032–3047.

(41) Stjernschantz, E.; Marelius, J.; Medina, C.; Jacobsson, M.; Vermeulen, N. P. E.; Oostenbrink, C. Are automated molecular dynamics simulations and binding free energy calculations realistic tools in lead optimization? An evaluation of the linear interaction energy (LIE) method. *J. Chem. Inf. Model.* **2006**, *46*, 1972–1983.

(42) Warren, G. L.; Andrews, C. W.; Capelli, A. M.; Clarke, B.; LaLonde, J.; Lambert, M. H.; Lindvall, M.; Nevins, N.; Semus, S. F.; Senger, S.; Tedesco, G.; Wall, I. D.; Woolven, J. M.; Peishoff, C. E.; Head, M. S. A critical assessment of docking programs and scoring functions. *J. Med. Chem.* **2006**, *49*, 5912–5931.

(43) Lewis, D. F.; Lake, B. G. Molecular modelling of CYP1A subfamily members based on an alignment with CYP102: rationalization of CYP1A substrate specificity in terms of active site amino acid residues. *Xenobiotica* **1996**, *26*, 723–753.

(44) Liu, G.; Gelboin, H. V.; Myers, M. J. Role of cytochrome P450 IA2 in acetanilide 4-hydroxylation as determined with cDNA expression and monoclonal antibodies. *Arch. Biochem. Biophys.* **1991**, *284*, 400–406.

(45) Venkatakrishnan, K.; von Moltke, L. L.; Greenblatt, D. J. Application of the relative activity factor approach in scaling from heterologously expressed cytochromes p450 to human liver microsomes: studies on amitriptyline as a model substrate. *J. Pharmacol. Exp. Ther.* **2001**, *297*, 326–337.

(46) Johne, A.; Perloff, E. S.; Bauer, S.; Schmider, J.; Mai, I.; Brockmoller, J.; Roots, I. Impact of cytochrome P-450 inhibition by cimetidine and induction by carbamazepine on the kinetics of hypericin and pseudohypericin in healthy volunteers. *Eur. J. Clin. Pharmacol.* **2004**, *60*, 617–622.

(47) Kariya, S.; Isozaki, S.; Uchino, K.; Suzuki, T.; Narimatsu, S. Oxidative metabolism of flunarizine and cinnarizine by microsomes from B-lymphoblastoid cell lines expressing human cytochrome P450 enzymes. *Biol. Pharm. Bull.* **1996**, *19*, 1511–1514.

(48) Pirmohamed, M.; Williams, D.; Madden, S.; Templeton, E.; Park, B. K. Metabolism and bioactivation of clozapine by human liver in vitro. *J. Pharmacol. Exp. Ther.* **1995**, *272*, 984–990.

(49) Yamazaki, H.; Shaw, P. M.; Guengerich, F. P.; Shimada, T. Roles of cytochromes P450 1A2 and 3A4 in the oxidation of estradiol and estrone in human liver microsomes. *Chem. Res. Toxicol.* **1998**, *11*, 659–665.

(50) Burke, M. D.; Mayer, R. T. Ethoxyresorufin: direct fluorimetric assay of a microsomal O-dealkylation which is preferentially inducible by 3-methylcholanthrene. *Drug Metab. Dispos.* **1974**, *2*, 583–588.

(51) Imaoka, S.; Enomoto, K.; Oda, Y.; Asada, A.; Fujimori, M.; Shimada, T.; Fujita, S.; Guengerich, F. P.; Funae, Y. Lidocaine metabolism by human cytochrome P-450s purified from hepatic microsomes: comparison of those with rat hepatic cytochrome P-450s. *J. Pharmacol. Exp. Ther.* **1990**, *255*, 1385–1391.

(52) Labbe, L.; Abolfathi, Z.; Lessard, E.; Pakdel, H.; Beaune, P.; Turgeon, J. Role of specific cytochrome P450 enzymes in the N-oxidation of the antiarrhythmic agent mexiletine. *Xenobiotica* **2003**, *33*, 13–25.

(53) Tracy, T. S.; Marra, C.; Wrighton, S. A.; Gonzalez, F. J.; Korzekwa, K. R. Involvement of multiple cytochrome P450 isoforms in naproxen O-demethylation. *Eur. J. Clin. Pharmacol.* **1997**, *52*, 293–298.

(54) Kinzig-Schippers, M.; Fuhr, U.; Zaigler, M.; Dammeyer, J.; Rusing, G.; Labedzki, A.; Bulitta, J.; Sorgel, F. Interaction of pefloxacin and enoxacin with the human cytochrome P450 enzyme CYP1A2. *Clin. Pharmacol. Ther.* **1999**, *65*, 262–274.

(55) Yun, C. H.; Miller, G. P.; Guengerich, F. P. Rate-determining steps in phenacetin oxidations by human cytochrome P450 1A2 and selected mutants. *Biochemistry* **2000**, *39*, 11319–11329.

(56) Ching, M. S.; Bichara, N.; Blake, C. L.; Ghabrial, H.; Tukey, R. H.; Smallwood, R. A. Propranolol 4- and 5-hydroxylation and N-desisopropylation by cloned human cytochrome P4501A1 and P4501A2. *Drug Metab. Dispos.* **1996**, *24*, 692–694.

(57) Rettie, A. E.; Korzekwa, K. R.; Kunze, K. L.; Lawrence, R. F.; Eddy, A. C.; Aoyama, T.; Gelboin, H. V.; Gonzalez, F. J.; Trager, W. F. Hydroxylation of warfarin by human cDNA-expressed cytochrome P-450: a role for P-4502C9 in the etiology of (S)-warfarin-drug interactions. *Chem. Res. Toxicol.* **1992**, *5*, 54–59.

(58) Spaldin, V.; Madden, S.; Adams, D. A.; Edwards, R. J.; Davies, D. S.; Park, B. K. Determination of human hepatic cytochrome P4501A2 activity in vitro use of tacrine as an isoenzyme-specific probe. *Drug Metab. Dispos.* **1995**, *23*, 929–934.

(59) Vickers, A. E.; Sinclair, J. R.; Zollinger, M.; Heitz, F.; Glanzel, U.; Johanson, L.; Fischer, V. Multiple cytochrome P-450s involved in the metabolism of terbinafine suggest a limited potential for drug-drug interactions. *Drug Metab. Dispos.* **1999**, *27*, 1029–1038.

(60) Machinist, J. M.; Mayer, M. D.; Shet, M. S.; Ferrero, J. L.; Rodrigues, A. D. Identification of the human liver cytochrome P450 enzymes involved in the metabolism of zileuton (ABT-077) and its N-dehydroxylated metabolite, Abbott-66193. *Drug Metab. Dispos.* **1995**, *23*, 1163–1174.

CI800371F